Molecularly Targeted Lanthanide Nanoparticles for Cancer Treatment

Subjects: Radiology, Nuclear Medicine & Medical Imaging

Contributor: Guillermina Ferro-Flores, Alejandra Ancira-Cortez, Blanca Ocampo-García, Laura Meléndez-Alafort

Injectable colloidal solutions of lanthanide oxides (nanoparticles between 10 and 100 nm in size) have demonstrated high biocompatibility and no toxicity when the nanoparticulate units are functionalized with specific biomolecules that molecularly target various proteins in the tumor microenvironment. Among the proteins successfully targeted by functionalized lanthanide nanoparticles are folic receptors, fibroblast activation protein (FAP), gastrin-releasing peptide receptor (GRP-R), prostate-specific membrane antigen (PSMA), and integrins associated with tumor neovasculature. Lutetium, samarium, europium, holmium, and terbium, either as lanthanide oxide nanoparticles or as nanoparticles doped with lanthanide ions, have demonstrated their theranostic potential through their ability to generate molecular images by magnetic resonance, nuclear, optical, or computed tomography imaging. Likewise, photodynamic therapy, targeted radiotherapy (neutron-activated nanoparticles), drug delivery guidance, and image-guided tumor therapy are some examples of their potential therapeutic applications.

Keywords: lanthanides ; nanoparticles ; targeting nanoparticles ; nanoparticle toxicity

1. Introduction

The group of lanthanides has been of interest for decades because of their luminescent properties [1][2]. In contrast to the other metals used to prepare nanoparticles, lanthanides are mostly found as dopant ions (Ln^{3+}) in core–shell nanostructures and as pure lanthanide oxides [2][3][4][5][6]. Lanthanide nanoparticles (LnNPs) are suitable to be used as pharmaceutical forms for theranostic applications in cancer. For this purpose, LnNPs must be colloidally stable in biological fluids, exhibit negligible uptake in healthy cells and tissues, and have functional groups on their surface attached to antibodies, peptides, biomolecules, or ligands that provide specific molecular targeting to proteins present in the tumor microenvironment (TME) [4][5][6].

In the pharmaceutical industry, a colloidal system is defined as a system consisting of two or more phases, one of which is a fluid (liquid), and the other is dispersed in the form of fine solid particles. The constant Brownian motion of each dispersed particle surrounding the solvent shell is responsible for the stability of such colloidal solutions. Nanocolloids are high-molecular-weight particles (size 10–100 nm) that have difficulty crossing capillary membranes in healthy tissues (with an opening between endothelial cells of 2 nm), making them ideal for accumulation in tumors, where the intercellular space of the vascular endothelium opens up to 400 nm [7].

The size and surface properties of LnNPs can be easily modified to obtain stable colloidal solutions that meet pharmaceutical requirements. The multifunctionalization of LnNPs is a relevant advantage when used as molecular targeting probes, since TME is formed by a complex network of proteins/peptides/small molecules and immune cells, fibroblasts and cancer cells, all of which are potential diagnostic/therapeutic targets. The functionalization of nanoparticles confers high molecular affinity by creating multiple ligand binding sites on the nanosurface, which is necessary for targeting specific proteins expressed in TME.

The surface of LnNPs determines their interaction with body systems when administered in vivo, so when coated with biomolecules, they are not recognized as foreign by the immune system and are not toxic.

Lanthanide-based nanomaterials offer multimodal approaches to diagnostics and therapeutics due to their magnetic, relaxivity, optical, and nuclear emission properties. The multifunctionality of LnNPs lies in their ability to provide diagnostic imaging of primary and metastatic tumors and their utility in photodynamic therapy, targeted radiotherapy (neutron-activated nanoparticles), drug delivery, and image-guided tumor surgery [8][9][10][11][12].

2. Physical Properties of Lanthanide-Based Nanoparticles for Theranostics

Metal nanoparticles (1–100 nm) have an extensive range of applications in biomedicine due to their physicochemical properties. They are utilized as targeted drug delivery, biosensors, as well as diagnostic and therapeutic agents for diseases like cancer. Therefore, an essential aspect is the synthesis route to achieve both the desired size and morphology. Additionally, these features are the starting point for successful surface modification and functionalization. The most effective methods for synthesizing these compounds include coprecipitation, solvothermal synthesis, thermal decomposition, microemulsion techniques, and wet-based chemistry methods [4][13].

The rare earth elements, also known as the lanthanides, are members of group IIIB of the periodic table, from Ln to Lu. Their electronic configuration can be denoted as $[Xe]4f^{(1-14)}5d^{(0-1)}6s^2$, which implies that the 4f orbital is partially filled, except for lanthanum ($[Xe]4f^0$) and lutetium ($[Xe]4f^{14}$). The 4f electrons are responsible for the special properties of rare earths, including enhanced electronic, magnetic, and optical properties at the nanometer scale. Ln^{3+} is the most stable and frequently observed oxidation state for these elements [4][13][14][15].

Optically, these properties are favored by the large quantum numbers (n = 4, l = 3), which create partially allowed intraconfigurations at the 4f level and are further shielded from environmental effects by the screening effect of the electrons at higher energy levels (5s and 5p). Therefore, these materials offer numerous advantages, such as numerous absorption bands with narrow emission profiles from the UV-Vis to the NIR, excellent photostability, large Stokes and anti-Stokes shifts, long luminescence half-lives (µm to ms), luminescence quantum efficiency, low background autofluorescence (practically zero), no photobleaching line-shaped emission, and low biotoxicity [2][15][16][17][18][19][20].

A theranostic molecule possesses unique and versatile properties that make it suitable for both therapy and diagnosis. Lanthanide-based nanoparticles (Ln-NPs) exhibit these characteristics. Depending on the nanoplatform design, one of the following scenarios may occur [5][6][21][22][23][24].

- Activation using near-infrared (NIR) light generates luminescence imaging for diagnostic purposes and triggers drug release for therapy.
- NIR activation also produces real-time luminescence imaging to evaluate the effectiveness of previously applied treatments for diagnosis and generates photothermal therapy (PTT) or photodynamic therapy (PDT).
- Neutron activation produces radioluminescence imaging with possible radiotherapy applications when beta particles are emitted.

Lanthanide nanoparticles include nanoparticles doped with lanthanide ions, alloys, metallic nanoparticles with varying percentages of lanthanides, lanthanide oxide nanoparticles, or core–shell nanoparticles [5][6][21][22][23][24].

2.1. Luminescence of Lanthanide-Doped Nanoparticles

Luminescence is a physical phenomenon generated by the movement of electrons contained in matter at different energy levels. It can be summarized as the absorption of energy to achieve an excited state which, upon returning to its basal state, releases this energy in the form of light, where the wavelength of the light emitted is a characteristic of the luminescent material and not of the incident radiation [17][21][25].

The luminescence of nanoparticles based on lanthanides occurs in the visible and NIR regions of the spectrum following stimulation by UV or NIR light. This phenomenon is further affected by both phonon energy and the strength of the crystal field that contains the Ln^{3+} ions. The use of Ln-NPs generates an optical image that enables visualization of subcellular morphological details and elucidation of signaling pathways and biological processes at the cellular level. Among the lanthanide ions, Eu^{3+}, Dy^{3+}, and Tb^{3+} exhibit the most effective luminescent characteristics [16][17][21][25].

2.2. Luminescence Emission Mechanisms

2.2.1. Downshifting

Downshift emission is a nonlinear Stokes-shift process. It is based on the absorption of a high energy, short wavelength photon (NIR-I photon), which is emitted as a lower energy, longer wavelength photon (NIR-II photon), producing luminescence. The mechanism is based on the direct excitation of photons to an E2 state and then to an E1 relaxation state with the emission of nonradiative energy. Finally, it reaches the E0 state, its initial state, with the emission of

luminescence. The nonradiative relaxation (E2→E1) is a multiphonon-assisted process governed by phonon dynamics. The generated emissions fall in the optical window between 700–1100 nm. These emissions can be of two types:

- Conversion of UV into visible light: The lanthanide ions representative of this emission are Er^{3+} (red emitter) and Tb^{3+} (green emitter).
- Conversion from UV-Vis to NIR: The lanthanide ions representative of this emission are Yb^{3+}, Nd^{3+} and Dy^{3+}.

In this process, as in the upconversion process, the structure and composition of the material, such as size, distribution, shape, and crystal phase, have a direct relationship to the quality and quantity of emitted luminescence [26][27][28][29][30].

2.2.2. Upconversion

The upconversion process was first termed the infrared quantum counter in 1959. It is an anti-Stokes emission and a non-linear optical phenomenon. This process involves the absorption of two or more low-energy photons to produce the emission of higher-energy photons (shorter wavelength) to the incident photon via a high-duration energetic state [2][16][18][31].

Upconversion emissions result from four distinct energy transfer pathways: excited-state absorption (ESA), energy transfer upconversion (ETU), cooperative energy transfer (CET), and energy migration-mediated upconversion (EMU) [2][16][31][32][33].

- ESA: This process involves sequential absorption of two or more low-energy photons by a single type of Ln^{3+} ion with medium-length energy states.
- ETU: In this process, there are two different luminescent centers, a sensitizer, and an activator. After excitation with a photon pump, energy is transferred from the sensitizer to the activator.
- CET: The photons generated have energies almost twice the transition energy. The emission energy originates from a significant disparity between the basal and the first excited state of the Ln^{3+} ion.
- EMU: In the core–shell structures, this procedure implicates four luminescent centers, including the sensitizer, activator, accumulator, and migrator. Energy is transferred consecutively across the interface of the core–shell.

The efficiency and process of upconversion exhibit high variation due to the varying energy levels in the 4f-4f intra-configurations. The complexity of these energy differences arises from the potential orbital-spin couplings of electrons and their interaction with the crystal field, resulting in process variations. Another influencing factor is the macrometric size (bulk material), where the absorption cross-section of the Ln^{3+} ions is small, which also generates a limited emission upconversion efficiency [25][31].

Lanthanide-based upconversion nanoparticles (Ln-based UCNPs) have improved the emission process, taking into account critical factors: (a) The symmetry of the Ln^{3+} ion in the crystal structure has been exploited to facilitate intraconformational transitions, with ions of smaller ionic radius than the lanthanoids strategically placed in the crystal; (b) Passivation of the surface of core–shell structures in order to minimize the quenching effect due to surface defects; (c) Modulation of transfer energy to reduce non-radiative losses and enhance radiative emission is ideal.

Ln-based UCNPs effectively transform various photons from the near-infrared (NIR) region, with low energy, into high-energy NIR, visible, or ultraviolet photon emissions [19][21]. Excitation with near-infrared (NIR) light (980–808 nm) within the biological optical window (700–1000 nm) enables deeper penetration into biological tissues and subsequent imaging with high sensitivity. Excitation with this light produces minimal autofluorescence because the NIR light does not excite fluorophores in the organism, resulting in a near-zero signal-to-noise ratio [2][5][17][18][19][20][21][34]. These systems serve as therapeutics through three approaches:

- Photodynamic therapy (PDT): a non-invasive therapy for cancer treatment with three essential components—light, photosensitizer, and oxygen. PDT involves the NIR light irradiation of UCNPs to generate upconversion emission, which excites the photosensitizer (PS). Subsequently, the energy from the excited PS is transferred to nearby triplet oxygens ($3O_2$), resulting in the creation of singlet-type reactive oxygen species (ROS) responsible for damaging cancer cells (O_3). This therapy yields better effects at shorter distances between the activator donor (energy donor) and the PS (energy acceptor); it is low-cost, accurate, and has minimal long-term side effects [5][16][19][21].

- Photothermal therapy (PTT): Therapy that converts light into heat to generate local hyperthermia to cause cancer cell death. The therapy is typically generated using AuNPs, organic dyes, graphene oxides, or QDs [5]. Its mechanism is based on multiphoton relaxation of the excited states of trivalent Ln^{3+} ions, combined with emission quenching effects generated by nonradiative centers located in the periphery [5][21].

- Drug delivery and therapy: Ln-based UCNPs enable drug delivery and release from drug-carrying platforms by functioning as high-penetration probes without interfering with the therapeutic process of the drugs. Additionally, photoactivation or photorelease at specific sites following noninvasive stimulation of the UCNPs with light, triggers drug release. The major advantage of the therapy is the use of NIR light, which avoids unwanted phototoxic tissue damage, in contrast to the use of UV light [16].

2.2.3. Quantum Cutting

This phenomenon is based on the absorption of high-energy photons emitted as two or more lower-energy photons. The efficiency of this phenomenon is greater than 100%. An example of this emission is presented by co-doped lanthanide compounds Gd^{3+} or Yb^{3+}/Tb^{3+}, Pr^{3+}, Ho^{3+} or Dy^{3+}.

Gd^{3+} or Yb^{3+} are the acceptor ions that emit luminescence by transferring energy to one of the complementary ions by multiphoton relaxation in the NIR. An option for this structure is hybrid NPs (organic–inorganic) with a sensitizer to absorb UV light. It can be said that this process is a mixture of downconversion and upconversion mechanisms.

2.3. Photoluminescence

The primary restriction of Ln-based NPs for generating luminescence is the low absorption coefficient of lanthanide ions. While the proximity and concentration of the Ln^{3+} ions are enhanced by nanometer size, incorporating sensitizing molecules is the best approach to increase the absorption coefficient. These molecules usually form stable complexes by binding to the Ln^{3+} ions. They efficiently absorb excitation energy, which is then transferred to the lanthanide ion when it returns to its basal state. The lanthanide ion uses this transferred energy to generate luminescence [35][36].

If the sensitizing molecules are organic, their absorption efficiency is due to the presence of π bonds, and the energy is absorbed through π–π* transitions. Conversely, if they are inorganic molecules (e.g., phosphonates), their absorption efficiency is mainly due to dipole–dipole, dipole–magnetic, or dipole–electric transitions [35][37].

2.4. Radioluminescence

X-rays are high-energy electromagnetic radiation with short wavelengths and high penetrating power. They are currently used for X-ray imaging as a low-cost, high-availability diagnostic tool. However, one of its major drawbacks is that it provides a two-dimensional image, which results in loss or lack of relevant information. In other words, the technique has low sensitivity [38][39].

On the other hand, when ionizing radiation interacts with specific materials, it can produce radioluminescent optical photons. Materials with a high atomic number have demonstrated the greatest efficacy due to their ability to absorb X-rays. This interaction can generate Cerenkov radiation, interact with scintillators, and induce fluorescence, phosphorescence, and luminescence.

Nanoparticles, particularly those based on lanthanides, have gained attention as materials with potential for radioluminescence imaging. They are influenced by the presence of a significant number of atoms on their surface, as well as by the quantum confinement of electronic states and the area-to-surface ratio. The aforementioned results in an increase in the interaction rate between ionizing radiation and ions, leading to more efficient radioluminescence generation despite their small size. Chemically, the high-Z, cross section, and high crystallinity of the ions are critical factors that enhance X-ray absorption and subsequent conversion into UV or NIR light.

Regarding the therapeutic use of radioluminescence, some reports describe the combination of scintillator materials with radiotherapy to promote photodynamic therapy [40][41][42][43]. The approach proposes converting X-rays to light via the use of a scintillator to activate the photosensitizer and achieve a therapeutic effect. The phenomenon's mechanism is described as relying on the transfer of Cerenkov radiation energy by a photon–photon or beta–photon emission interaction. The primary benefit of this approach is the restriction of additional dose radiation.

2.5. Fluorescence Imaging in the Second Near-Infrared Biological Window (NIR II 1000–1700 nm)

Optical stimulation in the near-infrared (NIR, 700–1700 nm) window has advantages in biomedical imaging because of its low absorption, low scattering, and minimal tissue autofluorescence, which is most evident in the NIR-II region (1000–1700 nm) [44][45].

NIR-II region is very close to zero at wavelengths longer than 1300 nm [46][47][48]. Chemically, the emitting and receiving electrons must conserve their spin moment to enable fluorescence emission. Physically, fluorescence is governed by the anti-Stokes shift phenomenon. NIR light excites the materials and produces emission in the NIR II region.

Some of the applications of fluorescence imaging with nanoparticles include gene detection, protein analysis, evaluation of enzyme activity, tracking of elements, diagnosis of early-stage diseases, and monitoring of therapeutic effects in real-time. The success of these applications is heavily reliant on several factors: (a) Employ excitation and emission wavelengths within the NIR region, preferably NIR-II, to enable deeper penetration of optical photons with less excitation damage to other components; (b) Implement systems with high biocompatibility and adequate functionalization and stability; (c) Ensure that fluorescence intensity and duration are maintained; (d) Avoid rapid scavenging when using nanoparticles. The appropriate size ranges from 5.5 to 150 nm, depending on the pathology to be analyzed [47][48].

Ln-based nanoparticles (NPs) can emit in NIR II (Stokes-shift-based imaging agents). This phenomenon is due to the optical and electronic properties of electrons in the 4f orbital. Host matrixes are the primary components, along with sensitizers and activators, where the latter two contain Ln^{3+} ions. These systems provide benefits such as deep tissue penetration, reduced background noise, and lower toxicity. Other features include high temporal resolution (20 ms), high spatial resolution, and high tissue penetration (up to 3 cm) [28][41][43][46][49].

2.6. Magnetic Resonance Imaging

MRI is based on the net polarization of the nuclear spins of water protons in the presence of an intense magnetic field of 1.5 to 3T. Therefore, the magnetic properties of the contrast agent require the insertion of one or more metal centers with unpaired electrons [50]. Gadolinium, terbium, dysprosium, and holmium oxide nanoparticles are of particular interest because they have appreciable magnetic moments, which is useful for MRI [51]. Gd^{3+} ions have been widely used to produce molecular T1 contrast enhancement [50]. Many papers have been published on Gd^{3+}-based nanostructures of different composition, shape, and size. However, only a few of them have been functionalized with small molecules, such as folic acid [41][52], RGD, chlorotoxin and transactivator of transcription (TAT) peptides [53][54][55], and the anti-thrombomodulin antibody [56].

3. Modification of Lanthanide-Based Nanoparticles with Active Molecules for Theranostics

Lanthanide nanoparticles have been functionalized with various biomolecules to molecularly target different specific sites in the tumor microenvironment (**Figure 1**).

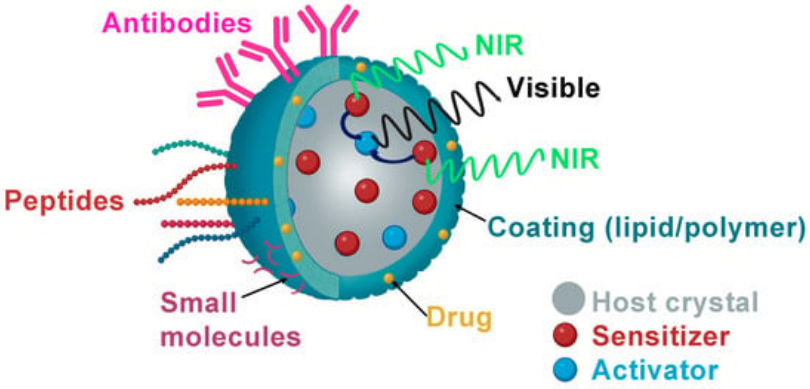

Figure 1. Schematic illustration of biological ligand-mediated targeted UCNPs that could be loaded with anticancer drugs as DOX and functionalized with small molecules as FA, peptides or antibodies.

3.1. Folic Acid (Small Molecules)

The first attempt to produce targeted NPs with biological molecules was made using stable and non-immunogenic small molecules such as folate or folic acid (FA), a water-soluble vitamin with a low molecular weight (411.4 Da). Folate

receptors are overexpressed on rapidly proliferating cells, such as cancer cells, due to their increased need for folate compared to normal cells. This overexpression in human tumors such as endometrial, breast, ovarian, and brain cancers can be used to target these tumors [57].

Cao et al. were the first to report water-soluble UCNPs functionalized with FA by introducing 6-aminohexanoic acid (AA) and oleate to control generation and crystal growth. AA was attached to the lanthanide ions through the carboxylic acid group, providing free amine groups that made the NPs dispersible in water and allowed conjugation with the FA. The UCNPs showed intense luminescence and helped obtain mouse lymphatic capillary imaging with a high signal-to-noise ratio. Their FA-functionalized UCNPs showed specific internalization in KB (FR-positive) cells, but the author did not test them in vivo [58].

Metal-organic frameworks (MOFs) are also promising candidates for drug delivery due to their microporous structure. UCNPs have been used to increase drug concentration at the tumor site by encapsulating molecules and rendering them biologically inert, thereby increasing chemotherapeutic efficacy and reducing toxicity and side effects for patients. By physical adsorption, Liu et al. synthesized PeGylated UCNPs loaded with the anticancer drug doxorubicin (DOX). They conjugated them with folic acid to evaluate the loading and release of DOX at different pH values. They found that 20% of DOX was released at physiological pH (7.4), with this rate increasing at lower pH values.

Mesoporous silica nanospheres (MSNs) have also been functionalized with FA for tumor targeting. Shi et al. reported MSNs loaded with Zn1.1Ga1.8Ge0.1O4:Cr^{3+}, Eu^{3+} to obtain persistent luminescent nanoparticles (PLNPs), which were modified with FA and subsequently loaded with DOX [59]. The DOX-NLPLNPs@MSNs-FA was evaluated as a real-time monitoring drug delivery agent.

Lanthanum oxide nanoparticles have also been used as optical devices in medicine. Recently, hafnium dioxide (HfO_2) NPs doped with Eu^{3+}, Gd^{3+}, and Tb^{3+} ions and functionalized with FA were synthesized by different routes to evaluate their potential as a matrix for multimodal theranostic agents for image-guided radiotherapy. The results showed that sol–gel-based synthesis was the best method to prepare uniformly doped particles with good size control. It was also demonstrated that introducing lanthanide ions could tune the luminescence, MR, and CT properties. Gd:HfO_2 NPs showed the best properties, such as the lowest degradation rate and no relevant in vitro cytotoxicity [60].

3.2. Peptides

Peptides are cancer-specific ligands with moderate size, high stability, and low immunogenicity but still possess a high specificity towards their target. Moreover, they are easy to synthesize on a large scale and modify; therefore, some peptides have been used to functionalize the NPs to be applied as image-guided tracking and also to direct chemical drug-loaded lanthanide nanoprobes to the tumor sites, achieving higher tumor inhibition than pristine drugs [9].

The most commonly used peptide to functionalize NPs is arginine-glycine-aspartic acid (RGD) because it can recognize the adhesion receptor integrin $\alpha_v\beta_3$, which is overexpressed on tumor endothelial cells [61]. Xiong et al. reported the first UCNPs doped with Yb, Er, and Tm and functionalized with RGD for fluorescence-targeted imaging in vivo. To improve the blood circulation of the nanosystem, the authors added a PEG linkage [62]. Confocal imaging of tissue sections at high penetration depths of these nanosystems showed that UCL imaging without an autofluorescence signal was possible. In addition, the experimental results in mice bearing human glioblastoma (U87MG) showed that the functionalization of this nanoplatform enables target-specific imaging of tumors with a high signal-to-noise ratio, making this technique also suitable for tracking in vivo components of biological systems.

Prostate-specific membrane antigen (PSMA protein) is an important molecular target due to its overexpression in various cancer cells, including advanced and metastatic prostate cancer. This has led to successfully generating radiolabeled PSMA inhibitor peptide (iPSMA) based systems as agents for molecular imaging and radiotherapy [23][63][64].

The iPSMA peptide has also been used to functionalize [^{166}Dy]Dy_2O_3, $^{166}Ho_2O_3$, and [^{177}Lu]Lu_2O_3 nanoparticles with utility as targeted radiotherapy systems [23][63][64]. Dysprosium and holmium oxide nanoparticles were reported as a novel in vivo generator. That is, [^{166}Dy]Dy_2O_3 NPs were obtained by neutron irradiation of $^{164}Dy_2O_3$ NPs, which decay to $^{166}Ho_2O_3$ NPs under a nuclear transient equilibrium. After functionalization with the iPSMA peptide, an in vivo [^{166}Dy]Dy_2O_3-iPSMA/$^{166}Ho_2O_3$-iPSMA generator for medical applications was obtained. In vitro and in vivo studies demonstrated the potential of this molecularly targeted lanthanide generator to deliver ablative radiation doses to HepG2 liver cancer cells [65].

On the other hand, chemical analysis of Lu_2O_3-iPSMA also resulted in a well-defined hemispherical shape with a uniform and monodispersed size distribution (30–45 nm) and characteristic radioluminescence features after neutron activation. The in vitro studies showed a high affinity of $^{177}Lu_2O_3$-PSMA for PSMA-expressing cells.

Fibroblast activation protein (FAP) has become one of the most important molecular targets involved in the tumor microenvironment [66]. Cancer-associated fibroblasts induce the cancer phenotype, account for 90% of the macroscopic tumor mass, and strongly express FAP in >90% of carcinomas. As a result, FAP is overexpressed in the neoplastic microenvironment of more than ninety percent of epithelial tumors and is a major contributor to cancer progression [66]. This is why Lu_2O_3 nanoparticles activated by neutron activation have also been functionalized with FAP inhibitor peptides (iFAP).

Bombesin can also be recognized by GRPr overexpressed in breast, prostate, lung, CNS, colon, and pancreatic tumors, where it functions as an autocrine growth factor [67]. Tang et al. first used bombesin to functionalize Gd^{3+}-loaded UCNPs and used it to obtain in vivo MRI, CT, and UCL images of prostate tumors [68].

3.3. Antibodies

Several antibodies or antigens have been attached to lanthanide nanoparticles to produce luminescent images and/or targeted radiotherapy. In these approaches, the role of antibodies is primarily to target approaches to the interested tissue through specific recognition. In these terms, antibody-functionalized lanthanide-doped CaF_2 biolabel for cancer cell targeting was synthesized by Sasidharan et al. They prepared monodispersed lanthanide (Eu^{3+}) doped CaF_2 nanoparticles and functionalized them with anti-EGFR through EDC-NHS coupling chemistry for specific binding to EGFR-overexpressing cells. The nanoparticles exhibited strong fluorescence emission at 612 nm [69]. EGFR overexpression has also been used to enable specific binding of functionalized UNPs (anti-EGFR-UNPs) for imaging modalities to achieve three-dimensional functional tissue imaging based on laser scanning in cancer cells [70].

Lanthanide nanoparticles functionalized with polyethyleneimine (PEI) and an antibody to detect alpha-fetoprotein (AFP) were also prepared. The positively charged PEI-PLNPs were bound to the negatively charged antibody-functionalized gold nanoparticles, forming an FRET inhibition probe. The persistent luminescence of the PEI-PLNPs was quenched in the presence of AFP but recovered when the AFP-specific antibodies were desorbed from the nanoparticles [71]. In a different nanoparticle–antibody system for targeted radiotherapy, the mAb-201b was conjugated to Au-coated lanthanide phosphate nanoparticles containing ^{177}Lu to target thrombomodulin receptors for pulmonary metastatic disease.

3.4. DNA/RNA and Aptamers

Attaching DNA/RNA to nanomaterials will enable nucleic acid-based assembly and drug delivery. RNA interference (RNAi) is a natural cellular process of post-transcriptional gene regulation that uses small, double-stranded RNAs to induce the controlled silencing of genes (siRNA). Therefore, by introducing siRNAs, we are able to harness the RNAi machinery for the therapeutic control of genes and the treatment of a variety of diseases [72][73][74].

For siRNA delivery, nanoparticles have been recently proposed as excellent approaches. siRNA can be incorporated into an NP formulation by covalently binding to NP components or by electrostatic interaction with the NP surface [75]. Coordination of lanthanides with phosphate groups and nucleobases is used to construct lanthanide-doped nanoparticles. The siRNA/$NaGdF_4$ nanoparticle system allowed siRNA to escape from the endosome for efficient gene silencing in vivo. In addition, siRNA targeting PD-L1 (siPD-L1) complexed with $NaGdF_4$ was able to block PD-L1 expression and thereby suppress tumor growth in mouse models of breast and colon cancer [76].

4. Theranostic Lanthanide Nanoparticles with Potential for Clinical Translation

The stability of the colloidal solution is the first requirement for the clinical translation of the different theranostic nanosystems of LnNPs as stable, effective, and safe drug forms [77].

For the stability of LnNPs, repulsive forces must be generated by similar charges to prevent the coagulation of the colloidal particles. After preparing a nanocolloidal solution from which all ions are removed by dialysis, the particles agglomerate because the total surface area is reduced, the particle size increases, and the particles settle rapidly. Therefore, the presence of electrolytes that provide some electrical charge is always necessary. However, the number of electrolytes must be limited to the amount that the colloids can adsorb, since an excess reduces the zeta potential by

accumulating ions opposite to the charge of the LnNPs. Therefore, the number of electrolytes should be sufficient to keep the zeta potential below a critical level [78].

The stability of nanoparticles as a pharmaceutical form with high zeta potential values is a prerequisite for their in vivo application. However, interactions with components of biological fluids, such as proteins, electrolytes, and small molecules, influence their electrical potential and reduce the absolute value of the zeta potential, although without affecting the stability of the nanosystems when coated with biomolecules covalently bound to their surface, which guarantees colloidal stability [23].

The development of efficient processes that meet the good manufacturing practices (GMP) requirements of regulatory authorities is one of the most important current challenges in the production of theranostic nanoparticles for use in patients. Biomolecule-coated LnNPs can be produced under GMP procedures as sterilized colloidal liquids with the quality characteristics of a clinical-grade formulation [6].

The toxicity associated with nanoparticles varies depending on their intrinsic composition, shape and size, surface area, surface layer, and in vivo stability [79]. The mechanism of nanoparticle toxicity is based on their ability to generate cytotoxic and genotoxic reactive species related to immune-mediated effects (inflammation) and oxidative stress [80]. Among the most studied are the toxic effects of metal nanoparticles on tissues. Since the main uptake of nanoparticles is by hepatic Kupffer cells and splenic macrophages, they have been described to induce hepatic dysfunction and structural changes related to, for example, increased levels of interleukin-1β and interleukin-6, pro-inflammatory cytokines, as well as increased alkaline phosphatase, liver enzyme aspartate aminotransferase (AST) and alanine aminotransferase (ALT) [81][82][83][84].

As an interesting case, preclinical results have shown that Lu_2O_3-iPSMA/-iFAP nanoparticles activated by neutron irradiation inhibit colorectal HCT116 tumor progression due to a combination of radiotherapy, prolonged tumor retention, and molecular recognition of iPSMA and iFAP, which made possible the in vivo tumor optical and nuclear imaging. There was no liver and renal toxicity evidence since negligible uptake values in non-target tissues were observed. The first clinical case of a patient with colorectal liver metastases was the proof-of-concept showing the selective uptake of the LnNPs by liver metastases but not in the liver parenchyma (**Figure 2**) [5].

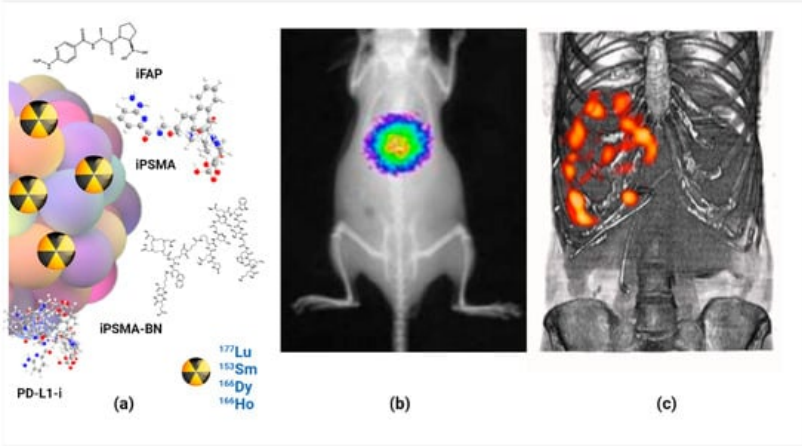

Figure 2. Schematic illustration of (**a**) molecularly targeted lanthanide nanoparticles for (**b**) optical imaging, (**c**) nuclear imaging and targeted radiotherapy (theranostics) of malignant tumors; observe the selective uptake of radiolanthanide lutetium oxide nanoparticles in colorectal liver metastases with negligible uptake in the liver parenchyma.

References

1. Wu, S.-Y.; Guo, X.-Q.; Zhou, L.-P.; Sun, Q.-F. Fine-tuned visible and near-infrared luminescence on self-assembled lanthanide-organic tetrahedral cages with triazole-based chelates. Inorg. Chem. 2019, 58, 7091–7098.
2. Dong, H.; Du, S.-R.; Zheng, X.-Y.; Lyu, G.-M.; Sun, L.-D.; Li, L.-D.; Zhang, P.-Z.; Zhang, C.; Yan, C.-H. Lanthanide nanoparticles: From design toward bioimaging and therapy. Chem. Rev. 2015, 115, 10725–10815.
3. Zheng, B.; Fan, J.; Chen, B.; Qin, X.; Wang, J.; Wang, F.; Deng, R.; Liu, X. Rare-earth doping in nanostructured inorganic materials. Chem. Rev. 2022, 122, 5519–5603.

4. Tegafaw, T.; Liu, Y.; Ho, S.L.; Liu, S.; Ahmad, M.Y.; Al Saidi, A.K.A.; Zhao, D.; Ahn, D.; Nam, H.; Chae, W.-S. High-Quantum-Yield Ultrasmall Ln2O3 (Ln = Eu, Tb, or Dy) Nanoparticle Colloids in Aqueous Media Obtained via Photosensitization. Langmuir 2023, 39, 15338–15342.
5. Luna-Gutiérrez, M.; Ocampo-García, B.; Jiménez-Mancilla, N.; Ancira-Cortez, A.; Trujillo-Benítez, D.; Hernández-Jiménez, T.; Ramírez-Nava, G.; Hernández-Ramírez, R.; Santos-Cuevas, C.; Ferro-Flores, G. Targeted Endoradiotherapy with Lu2O3-iPSMA/-iFAP Nanoparticles Activated by Neutron Irradiation: Preclinical Evaluation and First Patient Image. Pharmaceutics 2022, 14, 720.
6. Hernández-Jiménez, T.; Cruz-Nova, P.; Ancira-Cortez, A.; Gibbens-Bandala, B.; Lara-Almazán, N.; Ocampo-García, B.; Santos-Cuevas, C.; Morales-Avila, E.; Ferro-Flores, G. Toxicity Assessment of Lu− iFAP/iPSMA Nanoparticles Prepared under GMP-Compliant Radiopharmaceutical Processes. Nanomaterials 2022, 12, 4181.
7. Wu, J. The enhanced permeability and retention (EPR) effect: The significance of the concept and methods to enhance its application. J. Pers. Med. 2021, 11, 771.
8. Wei, Z.; Chao, Z.; Zhang, X.; Yu, J.; Xiao, F.; Zhang, X.; Tian, L. NIR-II Luminescent and Multi-Responsive Rare Earth Nanocrystals for Improved Chemodynamic Therapy. ACS Appl. Mater. Interfaces 2023, 15, 11575–11585.
9. Luo, Z.; Yi, Z.; Liu, X. Surface Engineering of Lanthanide Nanoparticles for Oncotherapy. Acc. Chem. Res. 2023, 56, 425–439.
10. Zhang, Q.; O'Brien, S.; Grimm, J. Biomedical applications of lanthanide nanomaterials, for imaging, sensing and therapy. Nanotheranostics 2022, 6, 184.
11. Godlewski, M.M.; Kaszewski, J.; Kielbik, P.; Olszewski, J.; Lipinski, W.; Slonska-Zielonka, A.; Rosowska, J.; Witkowski, B.S.; Gralak, M.A.; Gajewski, Z.; et al. New generation of oxide-based nanoparticles for the applications in early cancer detection and diagnostics. Nanotechnol. Rev. 2020, 9, 274–302.
12. Atabaev, T.S. Chapter 8—Multimodal inorganic nanoparticles for biomedical applications. In Nanobiomaterials in Medical Imaging; Grumezescu, A.M., Ed.; William Andrew Publishing: Norwich, NY, USA, 2016; pp. 253–278.
13. Pokhrel, M.; Burger, A.; Groza, M.; Mao, Y. Enhance the photoluminescence and radioluminescence of La2Zr2O7: Eu3+ core nanoparticles by coating with a thin Y2O3 shell. Opt. Mater. 2017, 68, 35–41.
14. Binnemans, K. Lanthanide-based luminescent hybrid materials. Chem. Rev. 2009, 109, 4283–4374.
15. Liu, B.; Li, C.; Yang, P.; Hou, Z.; Lin, J. 808-nm-Light-excited lanthanide-doped nanoparticles: Rational design, luminescence control and theranostic applications. Adv. Mater. 2017, 29, 1605434.
16. Kalyani, N.T.; Swart, H.C.; Dhoble, S.J. Principles and Applications of Organic Light Emitting Diodes (OLEDs); Woodhead Publishing: Sawston, UK, 2017.
17. Farka, Z.; Jurik, T.; Kovar, D.; Trnkova, L.; Skládal, P. Nanoparticle-based immunochemical biosensors and assays: Recent advances and challenges. Chem. Rev. 2017, 117, 9973–10042.
18. Pallares, R.M.; Abergel, R.J. Transforming lanthanide and actinide chemistry with nanoparticles. Nanoscale 2020, 12, 1339–1348.
19. Zhang, K.Y.; Yu, Q.; Wei, H.; Liu, S.; Zhao, Q.; Huang, W. Long-lived emissive probes for time-resolved photoluminescence bioimaging and biosensing. Chem. Rev. 2018, 118, 1770–1839.
20. Wang, Y.; Song, S.; Zhang, S.; Zhang, H. Stimuli-responsive nanotheranostics based on lanthanide-doped upconversion nanoparticles for cancer imaging and therapy: Current advances and future challenges. Nano Today 2019, 25, 38–67.
21. Yi, Z.; Luo, Z.; Qin, X.; Chen, Q.; Liu, X. Lanthanide-activated nanoparticles: A toolbox for bioimaging, therapeutics, and neuromodulation. Acc. Chem. Res. 2020, 53, 2692–2704.
22. Trujillo-Benítez, D.; Ferro-Flores, G.; Morales-Avila, E.; Jiménez-Mancilla, N.; Ancira-Cortez, A.; Ocampo-García, B.; Santos-Cuevas, C.; Escudero-Castellanos, A.; Luna-Gutiérrez, M.; Azorín-Vega, E. Synthesis and biochemical evaluation of samarium-153 oxide nanoparticles functionalized with iPSMA-bombesin heterodimeric peptide. J. Biomed. Nanotechnol. 2020, 16, 689–701.
23. Ancira-Cortez, A.; Ferro-Flores, G.; Jiménez-Mancilla, N.; Morales-Avila, E.; Trujillo-Benítez, D.; Ocampo-García, B.; Santos-Cuevas, C.; Escudero-Castellanos, A.; Luna-Gutiérrez, M. Synthesis, chemical and biochemical characterization of Lu2O3-iPSMA nanoparticles activated by neutron irradiation. Mater. Sci. Eng. C 2020, 117, 111335.
24. Kim, D.; Kim, J.; Park, Y.I.; Lee, N.; Hyeon, T. Recent development of inorganic nanoparticles for biomedical imaging. ACS Cent. Sci. 2018, 4, 324–336.
25. Han, S.; Deng, R.; Xie, X.; Liu, X. Enhancing luminescence in lanthanide-doped upconversion nanoparticles. Angew. Chem. Int. Ed. 2014, 53, 11702–11715.

26. Loo, J.F.-C.; Chien, Y.-H.; Yin, F.; Kong, S.-K.; Ho, H.-P.; Yong, K.-T. Upconversion and downconversion nanoparticles for biophotonics and nanomedicine. Coord. Chem. Rev. 2019, 400, 213042.

27. Yan, J.; Li, B.; Yang, P.; Lin, J.; Dai, Y. Progress in light-responsive lanthanide nanoparticles toward deep tumor theranostics. Adv. Funct. Mater. 2021, 31, 2104325.

28. Li, X.; Lu, S.; Tu, D.; Zheng, W.; Chen, X. Luminescent lanthanide metal–organic framework nanoprobes: From fundamentals to bioapplications. Nanoscale 2020, 12, 15021–15035.

29. Sudheendra, L.; Das, G.K.; Li, C.; Cherry, S.R.; Kennedy, I.M. Lanthanide-doped nanoparticles for hybrid x-ray/optical imaging. In Proceedings of the Reporters, Markers, Dyes, Nanoparticles, and Molecular Probes for Biomedical Applications V, San Francisco, CA, USA, 4–6 February 2013; pp. 76–83.

30. Cheignon, C.; Kassir, A.A.; Soro, L.K.; Charbonnière, L.J. Dye-sensitized lanthanide containing nanoparticles for luminescence based applications. Nanoscale 2022, 14, 13915–13949.

31. Kolobkova, E.; Mironov, L.Y.; Apanasevich, P.; Khodasevich, I.; Grabtchikov, A. Cooperative energy transfer as a probe of clustering in Yb3+ doped fluoroaluminate glasses. J. Lumin. 2023, 257, 119755.

32. Huang, H.; Wang, T.; Zhou, H.; Huang, D.; Wu, Y.; Zhou, G.; Hu, J.; Zhan, J. Luminescence, energy transfer, and up-conversion mechanisms of Yb3+ and Tb3+ co-doped LaNbO4. J. Alloys Compd. 2017, 702, 209–215.

33. Boschi, F.; Spinelli, A.E. Nanoparticles for Cerenkov and radioluminescent light enhancement for imaging and radiotherapy. Nanomaterials 2020, 10, 1771.

34. Lu, S.; Ke, J.; Li, X.; Tu, D.; Chen, X. Luminescent nano-bioprobes based on NIR dye/lanthanide nanoparticle composites. Aggregate 2021, 2, e59.

35. Kumar, P.; Creason, T.D.; Fattal, H.; Sharma, M.; Du, M.H.; Saparov, B. Composition-Dependent Photoluminescence Properties and Anti-Counterfeiting Applications of A2AgX3 (A = Rb, Cs; X = Cl, Br, I). Adv. Funct. Mater. 2021, 31, 2104941.

36. Liu, F.-Y.; Roces, L.; Sa, F.R.A.; Garca-Granda, S.; Garca, J.R.; Carlos, L.D.; Rocha, J. Crystal structure and photoluminescence properties of lanthanide diphosphonates. J. Mater. Chem. 2007, 17, 3696–3701.

37. Guryev, E.L.; Smyshlyaeva, A.S.; Shilyagina, N.Y.; Sokolova, E.A.; Shanwar, S.; Kostyuk, A.B.; Lyubeshkin, A.V.; Schulga, A.A.; Konovalova, E.V.; Lin, Q. UCNP-Based photoluminescent nanomedicines for targeted imaging and theranostics of cancer. Molecules 2020, 25, 4302.

38. Zhang, M.; Wang, X.; Yang, B.; Zhu, J.; Niu, G.; Wu, H.; Yin, L.; Du, X.; Niu, M.; Ge, Y. Metal halide scintillators with fast and self-absorption-free defect-bound excitonic radioluminescence for dynamic X-ray imaging. Adv. Funct. Mater. 2021, 31, 2007921.

39. Klein, J.S.; Sun, C.; Pratx, G. Radioluminescence in biomedicine: Physics, applications, and models. Phys. Med. Biol. 2019, 64, 04TR01.

40. Ancira-Cortez, A.; Trujillo-Benitez, D.; Jiménez-Mancilla, N.; Santos-Cuevas, C.; Morales-Avila, E.; Ferro-Flores, G. Synthesis and physicochemical characterization of Lu and Sm sesquioxide nanoparticles by precipitation-calcination and pulsed laser ablation in liquids. Mater. Chem. Phys. 2022, 275, 125229.

41. Cai, Q.; Wang, C.; Gai, S.; Yang, P. Integration of Au nanosheets and GdOF: Yb, Er for NIR-I and NIR-II light-activated synergistic theranostics. ACS Appl. Mater. Interfaces 2022, 14, 3809–3824.

42. Liu, L.; Shi, J.; Peng, S.; Zhong, H.; Lin, P.; Wang, J.; Sun, X.; Song, L.; Yuan, Q.; Zhang, Y. Biodegradable near-infrared-IIb lanthanide-doped inorganic nanoparticles with red up-conversion luminescence for bioimaging and photodynamic therapy. Sci. China Mater. 2023, 66, 2893–2901.

43. Zhong, Y.; Dai, H. A mini-review on rare-earth down-conversion nanoparticles for NIR-II imaging of biological systems. Nano Res. 2020, 13, 1281–1294.

44. Kudinov, K.; Bekah, D.; Cooper, D.; Shastry, S.; Hill, C.; Bradforth, S.; Nadeau, J. Lanthanum fluoride nanoparticles for radiosensitization of tumors. In Proceedings of the Colloidal Nanoparticles for Biomedical Applications XI, San Francisco, CA, USA, 13–15 February 2016; SPIE: Paris, France, 2016; pp. 109–116.

45. Jia, T.; Chen, G. Lanthanide nanoparticles for near-infrared II theranostics. Coord. Chem. Rev. 2022, 471, 214724.

46. Fan, Q.; Sun, C.; Hu, B.; Wang, Q. Recent advances of lanthanide nanomaterials in Tumor NIR fluorescence detection and treatment. Mater. Today Bio 2023, 20, 100646.

47. Ma, L.; Huang, S.; He, S.; Wang, Z.; Cheng, Z. Polydopamine-coated downconversion nanoparticle as an efficient dual-modal near-infrared-II fluorescence and photoacoustic contrast agent for non-invasive visualization of gastrointestinal tract in vivo. Biosens. Bioelectron. 2020, 151, 112000.

48. Kim, D.; Lee, N.; Park, Y.I.; Hyeon, T. Recent Advances in Inorganic Nanoparticle-Based NIR Luminescence Imaging: Semiconductor Nanoparticles and Lanthanide Nanoparticles. Bioconjugate Chem. 2017, 28, 115–123.

49. Bünzli, J.-C.G. Lanthanide luminescence: From a mystery to rationalization, understanding, and applications. In Handbook on the Physics and Chemistry of Rare Earths; Elsevier: Amsterdam, The Netherlands, 2016; Volume 50, pp. 141–176.

50. Banerjee, A.; Blasiak, B.; Dash, A.; Tomanek, B.; van Veggel, F.; Trudel, S. High-field magnetic resonance imaging: Challenges, advantages, and opportunities for novel contrast agents. Chem. Phys. Rev. 2022, 3, 011304.

51. Ahmad, M.Y.; Yue, H.; Tegafaw, T.; Liu, S.W.; Ho, S.L.; Lee, G.H.; Nam, S.W.; Chang, Y.M. Functionalized Lanthanide Oxide Nanoparticles for Tumor Targeting, Medical Imaging, and Therapy. Pharmaceutics 2021, 13, 21.

52. Cooper, D.R.; Capobianco, J.A.; Seuntjens, J. Radioluminescence studies of colloidal oleate-capped β-Na (Gd, Lu) F4: Ln3+ nanoparticles (Ln = Ce, Eu, Tb). Nanoscale 2018, 10, 7821–7832.

53. Jin, J.F.; Xu, Z.H.; Zhang, Y.; Gu, Y.J.; Lam, M.H.W.; Wong, W.T. Upconversion Nanoparticles Conjugated with Gd3+-DOTA and RGD for Targeted Dual-Modality Imaging of Brain Tumor Xenografts. Adv. Healthc. Mater. 2013, 2, 1501–1512.

54. Ahmad, M.Y.; Ahmad, M.W.; Cha, H.; Oh, I.T.; Tegafaw, T.; Miao, X.; Ho, S.L.; Marasini, S.; Ghazanfari, A.; Yue, H.; et al. Cyclic RGD-Coated Ultrasmall Gd2O3 Nanoparticles as Tumor-Targeting Positive Magnetic Resonance Imaging Contrast Agents. Eur. J. Inorg. Chem. 2018, 2018, 3070–3079.

55. Ahmad, M.Y.; Cha, H.; Oh, I.T.; Tegafaw, T.; Miao, X.; Ho, S.L.; Marasini, S.; Ghazanfari, A.; Yue, H.; Chae, K.S. Synthesis, Characterization, and Enhanced Cancer-Imaging Application of Trans-activator of Transcription Peptide-conjugated Ultrasmall Gadolinium Oxide Nanoparticles. Bull. Korean Chem. Soc. 2018, 39, 435–441.

56. Sobol, N.; Sutherlin, L.; Cedrowska, E.; Schorp, J.; Rodríguez-Rodríguez, C.; Sossi, V.; Lattimer, J.; Miller, D.C.; Pevsner, P.; Robertson, J.D. Synthesis and targeting of gold-coated 177Lu-containing lanthanide phosphate nanoparticles—A potential theranostic agent for pulmonary metastatic disease. APL Bioeng. 2018, 2, 016101.

57. Sabu, A.; Lin, J.-Y.; Doong, R.-A.; Huang, Y.-F.; Chiu, H.-C. Prospects of an engineered tumor-targeted nanotheranostic platform based on NIR-responsive upconversion nanoparticles. Mater. Adv. 2021, 2, 7101–7117.

58. Cao, T.Y.; Yang, Y.; Gao, Y.A.; Zhou, J.; Li, Z.Q.; Li, F.Y. High-quality water-soluble and surface-functionalized upconversion nanocrystals as luminescent probes for bioimaging. Biomaterials 2011, 32, 2959–2968.

59. Shi, J.P.; Sun, X.; Li, J.L.; Man, H.Z.; Shen, J.S.; Yu, Y.K.; Zhang, H.W. Multifunctional near infrared-emitting long-persistence luminescent nanoprobes for drug delivery and targeted tumor imaging. Biomaterials 2015, 37, 260–270.

60. Gerken, L.R.H.; Keevend, K.; Zhang, Y.C.; Starsich, F.H.L.; Eberhardt, C.; Panzarasa, G.; Matter, M.T.; Wichser, A.; Boss, A.; Neels, A.; et al. Lanthanide-Doped Hafnia Nanoparticles for Multimodal Theranostics: Tailoring the Physicochemical Properties and Interactions with Biological Entities. Acs Appl. Mater. Interfaces 2019, 11, 437–448.

61. Bolzati, C.; Salvarese, N.; Carpanese, D.; Seraglia, R.; Meléndez-Alafort, L.; Rosato, A.; Capasso, D.; Saviano, M.; Del Gatto, A.; Comegna, D.; et al. 99mTc Tc(N)PNP43 -Labeled RGD Peptides As New Probes for a Selective Detection of αvβ3 Integrin: Synthesis, Structure-Activity and Pharmacokinetic Studies. J. Med. Chem. 2018, 61, 9596–9610.

62. Xiong, L.Q.; Chen, Z.G.; Tian, Q.W.; Cao, T.Y.; Xu, C.J.; Li, F.Y. High Contrast Upconversion Luminescence Targeted Imaging in Vivo Using Peptide-Labeled Nanophosphors. Anal. Chem. 2009, 81, 8687–8694.

63. Brunello, S.; Salvarese, N.; Carpanese, D.; Gobbi, C.; Melendez-Alafort, L.; Bolzati, C. A review on the current state and future perspectives of Tc-housed PSMA-i in prostate cancer. Molecules 2022, 27, 2617.

64. Ferro-Flores, G.; Luna-Gutiérrez, M.; Ocampo-García, B.; Santos-Cuevas, C.; Azorín-Vega, E.; Jiménez-Mancilla, N.; Orocio-Rodríguez, E.; Davanzo, J.; García-Pérez, F.O. Clinical translation of a PSMA inhibitor for 99mTc-based SPECT. Nucl. Med. Biol. 2017, 48, 36–44.

65. Canseco-Hernández, O.; Ferro-Flores, G.; Jimenez-Mancilla, N.; Aranda-Lara, L.; Ocampo-Garcia, B.; Trujillo-Benitez, D.; Ancira-Cortés, A.; Morales-Avila, E.; Santos-Cuevas, C. Preparation and Dosimetry Assessment of 166Dy2O3/166Ho2O3-iPSMA Nanoparticles for Targeted Hepatocarcinoma Radiotherapy. J. Nanosci. Nanotechnol. 2021, 21, 5449–5458.

66. Vallejo-Armenta, P.; Ferro-Flores, G.; Santos-Cuevas, C.; García-Pérez, F.O.; Casanova-Triviño, P.; Sandoval-Bonilla, B.; Ocampo-García, B.; Azorín-Vega, E.; Luna-Gutiérrez, M. Tc-iFAP/SPECT tumor stroma imaging: Acquisition and analysis of clinical images in six different cancer entities. Pharmaceuticals 2022, 15, 729.

67. Moreno, P.; Ramos-Alvarez, I.; Moody, T.W.; Jensen, R.T. Bombesin related peptides/receptors and their promising therapeutic roles in cancer imaging, targeting and treatment. Expert Opin. Ther. Targets 2016, 20, 1055–1073.

68. Tang, S.H.; Wang, J.N.; Yang, C.X.; Dong, L.X.; Kong, D.L.; Yan, X.P. Ultrasonic assisted preparation of lanthanide-oleate complexes for the synthesis of multifunctional monodisperse upconversion nanoparticles for multimodal imaging. Nanoscale 2014, 6, 8037–8044.
69. Sasidharan, S.; Jayasree, A.; Fazal, S.; Koyakutty, M.; Nair, S.V.; Menon, D. Ambient temperature synthesis of citrate stabilized and biofunctionalized, fluorescent calcium fluoride nanocrystals for targeted labeling of cancer cells. Biomater. Sci. 2013, 1, 294–305.
70. Gainer, C.F.; Utzinger, U.; Romanowski, M. Scanning two-photon microscopy with upconverting lanthanide nanoparticles via Richardson-Lucy deconvolution. J. Biomed. Opt. 2012, 17, 076003.
71. Wu, B.-Y.; Wang, H.-F.; Chen, J.-T.; Yan, X.-P. Fluorescence resonance energy transfer inhibition assay for α-fetoprotein excreted during cancer cell growth using functionalized persistent luminescence nanoparticles. J. Am. Chem. Soc. 2011, 133, 686–688.
72. Afonin, K.A.; Viard, M.; Kagiampakis, I.; Case, C.L.; Dobrovolskaia, M.A.; Hofmann, J.; Vrzak, A.; Kireeva, M.; Kasprzak, W.K.; KewalRamani, V.N. Triggering of RNA Interference with RNA–RNA, RNA–DNA, and DNA–RNA Nanoparticles. In Therapeutic RNA Nanotechnology; Jenny Stanford Publishing: Singapore, 2021; pp. 681–705.
73. Chakraborty, C. Potentiality of small interfering RNAs (siRNA) as recent therapeutic targets for gene-silencing. Curr. Drug Targets 2007, 8, 469–482.
74. Senapati, D.; Patra, B.C.; Kar, A.; Chini, D.S.; Ghosh, S.; Patra, S.; Bhattacharya, M. Promising approaches of small interfering RNAs (siRNAs) mediated cancer gene therapy. Gene 2019, 719, 144071.
75. Morales-Becerril, A.; Aranda-Lara, L.; Isaac-Olivé, K.; Ocampo-García, B.E.; Morales-Ávila, E. Nanocarriers for delivery of siRNA as gene silencing mediator. EXCLI J. 2022, 21, 1028–1052.
76. Yu, C.; Li, K.; Xu, L.; Li, B.; Li, C.; Guo, S.; Li, Z.; Zhang, Y.; Hussain, A.; Tan, H.; et al. siRNA-functionalized lanthanide nanoparticle enables efficient endosomal escape and cancer treatment. Nano Res. 2022, 15, 9160–9168.
77. Stipic, F.; Pletikapić, G.; Jaksic, Z.; Frkanec, L.; Zgrablic, G.; Buric, P.; Lyons, D.M. Application of functionalized lanthanide-based nanoparticles for the detection of okadaic acid-specific immunoglobulin G. J. Phys. Chem. B 2015, 119, 1259–1264.
78. Ajdary, M.; Moosavi, M.A.; Rahmati, M.; Falahati, M.; Mahboubi, M.; Mandegary, A.; Jangjoo, S.; Mohammadinejad, R.; Varma, R.S. Health concerns of various nanoparticles: A review of their in vitro and in vivo toxicity. Nanomaterials 2018, 8, 634.
79. Ahmad, A. Safety and Toxicity Implications of Multifunctional Drug Delivery Nanocarriers on Reproductive Systems In Vitro and In Vivo. Front. Toxicol. 2022, 4, 895667.
80. Liu, F.; Chang, X.; Tian, M.; Zhu, A.; Zou, L.; Han, A.; Su, L.; Li, S.; Sun, Y. Nano NiO induced liver toxicity via activating the NF-κB signaling pathway in rats. Toxicol. Res. 2017, 6, 242–250.
81. Sha, B.; Gao, W.; Wang, S.; Gou, X.; Li, W.; Liang, X.; Qu, Z.; Xu, F.; Lu, T.J. Oxidative stress increased hepatotoxicity induced by nano-titanium dioxide in BRL-3A cells and Sprague–Dawley rats. J. Appl. Toxicol. 2014, 34, 345–356.
82. Yao, Y.; Zang, Y.; Qu, J.; Tang, M.; Zhang, T. The toxicity of metallic nanoparticles on liver: The subcellular damages, mechanisms, and outcomes. Int. J. Nanomed. 2019, 14, 8787–8804.
83. Sha, B.; Gao, W.; Wang, S.; Li, W.; Liang, X.; Xu, F.; Lu, T.J. Nano-titanium dioxide induced cardiac injury in rat under oxidative stress. Food Chem. Toxicol. 2013, 58, 280–288.
84. Teresa Pinto, A.; Laranjeiro Pinto, M.; Patrícia Cardoso, A.; Monteiro, C.; Teixeira Pinto, M.; Filipe Maia, A.; Castro, P.; Figueira, R.; Monteiro, A.; Marques, M. Ionizing radiation modulates human macrophages towards a pro-inflammatory phenotype preserving their pro-invasive and pro-angiogenic capacities. Sci. Rep. 2016, 6, 18765.